Hierarchical 3D-Printed Truss Structure with Global Stability Constraints

Yizhuo Liu*, Hao Hua

School of Architecture, Southeast University
2 Sipailou, Nanjing, China
liuyizhuo@seu.edu.cn

Abstract

We consider hierarchical truss optimization problems with a novel perspective on local and global stability, following the metamaterial paradigm of additive manufacturing. Using modular components for hierarchical truss fails to exploit the full mechanical potential, while geometric and topology optimization with structural hierarchy is a major challenge. Global stability analysis makes the optimization problem highly nonlinear and leads to nonconvex semidefinite programming. Given the unprecedent geometric flexibility of 3D metal printing, we propose the recursive construction of hierarchical truss across multiple scales, ranging from the building scale to the finest manufacturing resolution. By replacing an instable two-force member with a fusiform truss, the local buckling behavior characterized by Euler's critical load is transformed as the global buckling phenomenon associated with the positive semidefinite condition of geometrical stiffness matrix. Numerical examples demonstrate that hierarchical truss structures effectively save materials compared with conventional designs. The hierarchical truss is a promising prototype for the metamaterials under axial compression. Large-scale metal truss structures built with 3D-printed members could find multiple applications.

Keywords: Hierarchical Structure, Truss, Global Stability, Additive Manufacturing, Semidefinite Programming

1. Introduction

Many natural and artificial objects consist of structures on more than one scale [1]. A structural unit of these objects often has its own sophisticated structure. This structural hierarchy significantly influences the global behaviors of the material at a macroscopic level [2]. Hierarchical truss structures have been widely used in architecture and bridge design. One celebrated example is the Eiffel Tower [3]. Each truss member in the tower reveals itself as a smaller truss at a lower scale, and each sub-member within the lower-scale truss is another truss. Such fractal structure could facilitate practical construction by employing smaller members, and the resultant complex structure achieves efficiency of material use with desired strength [4].

Recent researches [5-7] have improved the mechanical efficiency of hierarchical structures. Under certain compliance constraint and without stability constraints, a solid slender rod is perfect as compressive two-force member. However, the rod needs to be stable against Euler's critical load when introducing the stability constraint. Such redesign process can be formulated as an optimization problem as follows. Given a compressive force F applied at two end points separated by a distance L, what geometry minimizes the volume V required to withstand F? A particular structure of fractal truss was proposed by Farr [8,9] to solve this problem, demonstrating its high efficiency subjected to compressive forces. Although manufactured through 3D printing with freeform geometry, their final structure is still composed of modular members, which limits the full potential of hierarchical structures.

Cutting-edge 3D printing technology enables scientists to create metamaterials with customized behaviors at each level of scales [10]. Multiscale materials with structural hierarchy have blurred the boundary between material science and structural engineering [11-13]. Given the unprecedent geometric

freedom from 3D metal printing [14], this research proposes a recursive process for hierarchical metal truss that covers multiple scales, ranging from the building scale (10 m) to manufacturing resolution (say 30 µm). Within the hierarchical truss structure, each smaller truss acting as a single member in its upper hierarchy should maintain a global buckling stability against expected axial loads, and each finest bar (at the bottom hierarchy) has to be stable against Euler buckling. We tackle global stability constraints with a linear buckling model formulated as a nonlinear semidefinite programming problem [15,16]. The model has been employed for advanced truss optimizations [17-19].

The paper is organized as follows. Section 2 presents the two optimization models and proposes the recursive construction method. Section 3 introduces numerical examples and a 3D-printed mock-up to demonstrate the feasibility of the proposed method, with comparison to conventional designs. Section 4 discusses the model limitations, metamaterials with additive manufacturing, and future works.

2. Methods

This section introduces the formulation of the truss optimization problems considering stability constraints. Two models for the minimum volume truss optimization are presented. One includes both local and global buckling constraints; the other only contains global buckling constraints. Integrating the two models leads to the recursive algorithm for hierarchical truss construction.

The truss structure in this work is treated as:
(1) a discrete assembly of two-forces bars connected by pinned joints. Its mechanical behavior can be modeled by a system of linear equations with the principles of statics and linear elasticity. The global stability is associated with the positive semidefinite conditions of its geometrical stiffness matrix.
(2) a continuum body of porous material with inner fractal structures, which is optimized for bearing axis compression. The local behaviors can be approximated as a linear bar or a fusiform truss.

2.1. Stability of Truss Structures

The geometry of the truss is defined by n nodes and m bars in the 3-dimensional Euclidean space. The design variables consist of the coordinates of the nodes v_i, for $i = 1, 2, ..., n$, and the cross-sectional areas a_j, for $j = 1, 2, ..., m$. The cross-sections of bars are circular. Let $c = 3n-n_0$, where n_0 denotes the number of fixed degrees of freedom.

Given an external load $F \in R^c$, the corresponding nodal displacement $u \in R^c$ follows the linear equilibrium equation:

$$K(a,v)u = F \tag{1}$$

Where $K(a, v)$ is the stiffness matrix (see Hutton [20] for details). The internal force f_j in the j-th bar is:

$$f_j = \frac{Ea_j}{l_j}\gamma_j u \tag{2}$$

Where E denotes the Young's modulus of the material, l_j and γ_j are the length and direction cosine vector of the j-th bar, respectively. The critical buckling load P_j of the j-th bar is given by Euler's formula [21]:

$$P_j = \frac{\pi^2 E I_j}{l_j^2} \tag{3}$$

Where I_j denotes the second moment of area of the cross section of the j-th bar. If the j-th bar is under compression (internal force f_j is negative), $|f_j| < P_j$ holds as the local stability constraint.

Besides individual bars, the truss itself should be strong enough concerning global buckling. We adopt the prebuckling model [17,18], which simplifies the relationship between displacements and applied loads near buckling. The model is formulated as a semidefinite programming problem:

$$K(a,v) + \lambda G(a,v,u) \succcurlyeq 0 \tag{4}$$

Where $G(a,v,u)$ is the so-called geometrical stiffness matrix:

$$G(a,v,u) = \sum_{j=1}^{M} \frac{a_j E \gamma_j u}{l_j^2}(\delta_j \delta_j^T + \eta_j \eta_j^T) \tag{5}$$

Where δ_j, η_j and γ_j form an orthogonal frame, the details for choosing vectors δ_j and η_j refer to Alexis [22] and Weldeyesus [23]. Constraint (4) ensures that the truss is stable under the load λF, which means that the given design load factor λ should be at least 1.

2.2 The Two Models for Truss Optimization

Model$_\alpha$ for the minimum volume optimization consists of both local and global stability constraints:

$$
\begin{aligned}
\underset{a,v}{\text{minimize}} \quad & \sum_{i=1}^{M} l_i a_i \\
\text{subject to} \quad & \zeta_{min} \leq F^T u \leq \zeta_{max} \\
& K(v,a) + \lambda G(v,a,u) \succcurlyeq 0 \\
& |f_i| \leq P_i, \quad if\ f_i < 0\ , \forall i = 1,2, \dots m \\
& f_i \leq \sigma_0 a_i\ , \quad \forall i = 1,2, \dots m \\
& a_i > 0, \quad \forall i = 1,2, \dots m
\end{aligned}
\tag{6}
$$

Where ζ_{min} and ζ_{max} are the given compliance bounds, σ_0 is the given stress limit related to the material.

The truss obtained by solving problem (6) yields an optimal truss of a single hierarchy. Subdividing its bars into smaller trusses cannot improve material efficiency, since the bars are already stable according to Euler's formula. Any subdivision variations actually reduce their stiffness using the same volume of materials.

To create a new design space for more efficient structure, model$_\beta$ treats the stability constraints across multiple scales. Removing local stability constraint ($|f_i| \leq P_i$) from problem (6) results in the optimization problem only concerning global stability. The optimal truss obtained by model$_\beta$ probably contains instable bars under compression. To achieve stability, any instable bar should either use bigger cross-sectional area (requiring additional material use) or be subdivided into a truss so that the local stability problem is transformed as the global stability problem at a lower scale.

2.3 Recursive Construction of Hierarchical Truss

This section introduces the recursive algorithm using model$_\alpha$ and model$_\beta$ to construct hierarchical truss. Let T denote a truss obtained by model$_\beta$, which contains instable members under compression. These linear members are further subdivided into new trusses to gain stability. Let b_j and t_j denote the *j*-th member and the new truss which replaces the *j*-th member in T, respectively.

Let f_j, l_j and a_j denote the internal force, length and cross-sectional area of b_j, respectively. Optimizing t_j as a free body requires data of b_j, including f_j, l_j and a_j. The new truss t_j contains the two end points of b_j, one of which is assumed as a freely hinged support during the free-body optimization. An axial compression force applied at the free end, which is equal in magnitude to f_j (considiered as the external load F_j of t_j). The stiffness k_j of b_j is computed as:

$$
k_j = \frac{a_j E}{l_j}
\tag{7}
$$

Truss t_j should maintain the same stiffness as bar b_j, (otherwise the structure will not comply with the compliance and global stability constraints). For ease of finding mathematical solution, its stiffness is allowed to fluctuate within a range of plus or minus 5%. The compliance bound ζ_{j-min} and ζ_{j-max} of t_j are:

$$
\zeta_{j-min} = 0.95\frac{f_j^2}{k_j},\ \zeta_{j-max} = 1.05\frac{f_j^2}{k_j}
\tag{8}
$$

The process of subdividing the instable members is concluded in Algorithm1.

$G_\alpha(T^\beta_i)$ and $G_\beta(T^\beta_i)$ produces T^α_{i+1} and T^β_{i+1}, respectively. T^α_{i+1} won't be subdivided as it is both locally and globally stable. While T^β_{i+1} will be processed by Algorithm1 again. This process continues until the minimum bar diameter approaches manufacturing limit. The stopping criterion is that the numbers of bars in T^β_i and T^β_{i+1} are the same. The feasible solution set of hierarchical truss includes T^α_1 to T^α_i, in

which the optimal structure is the one with minimal material volume. T^α_i is the *i*-th generation truss of the recursive algorithm. The recursive process is presented in Algorithm2 and Figure 1.

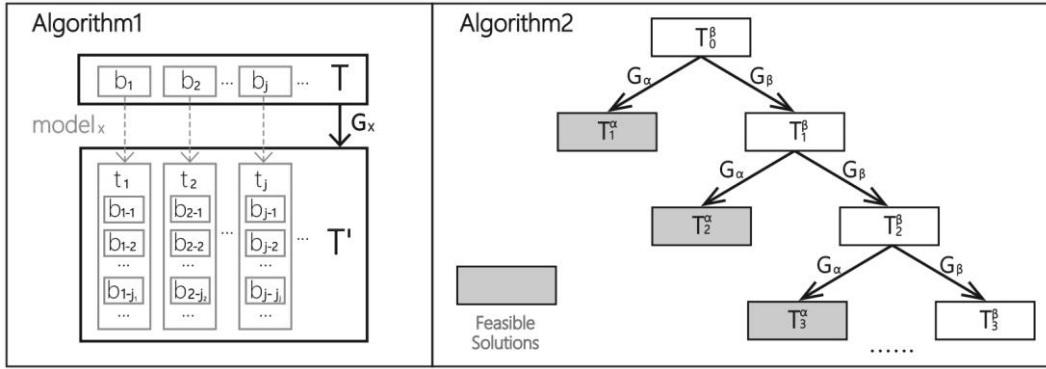| **Algorithm1** Subdivision Process of Instable Bars	**Algorithm2** Constructing Hierarchical Truss

$x \in \{\alpha, \beta\}$
$G_x(T)$:
    $T' \leftarrow \emptyset$
    For b_j in T:
        If b_j is instable under compression force:
            Use $model_x$ to optimize t_j
            Add t_j to T'
        Else:
            Add b_j to T'
    Return T'
	$i \leftarrow 0$
	$H(T^\beta_i)$:
	    $T^\alpha_{i+1} \leftarrow G_\alpha(T^\beta_i)$
	    $T^\beta_{i+1} \leftarrow G_\beta(T^\beta_i)$
	        If T^β_{i+1} contains more bars than T^β_i:
	            $H(T^\beta_{i+1})$:
	    Else
	        End

Figure 1: Recursive method for constructing hierarchical truss.

3 Numerical Experiments

This section presents two numerical experiments of hierarchical trusses to demonstrate the effectiveness of the recursive construction. One particular topology of truss replacing instable bars is introduced. This work assumes the material properties of titanium alloy TC4, a common material used in metal 3D printing [24] (E = 110 GPa, σ_0 =950 MPa). In all cases, the design load factor $\lambda = 1$, the manufacturing limit is 0.1mm.

3.1 Topology and Parametrization

For comparable analysis, the truss topology of Farr's research [9] is adopted to replace instable bar in the recursive process. The topology consists of a regular tetrahedron at each of its ends, with a series of *w* regular octahedra in between, as shown in Figure 2 for the case *w*=8. The structure contains *3w+5* nodes and *9w+9* members of equal length.

A compressive load F is applied to the two ends of the truss along the central axis. The bars parallel to the yz-plane (blue segments in Figure 2) are under tension; the rest members marked in red are under compression. Due to the symmetry between the truss and the compressive load, the coordinates of the nodes can be represented as the scaling triangles in yz-plane (in blue) and the distance between them. Let $d \in R+^{w+2}$ denote the distance between a pair of neighboring triangles in the yz-plane, and $s \in R+^{w+1}$ denotes the scaling ratio of the triangles. The value of $\sum_i^{w+2} d_i$ is fixed, and the reference point for scaling is located at the center of each triangle. The node coordinates v_i, $i = 1, 2, ..., 3w+5$, can be computed with variable *d* and *s*.

To better illustrate different structures derived from $model_\alpha$ and $model_\beta$, the numerical experiment of a single-hierarchy truss is conducted before the recursive subdivision.

Consider a truss with *w*=10 and a length of 1000mm. The equivalent stiffness *k*=600 N/mm remains unchanged and different external load *F* is tested. The compliance bound ζ is given by (8). Figure 3(a)

and Figure 3(b) show the results by model$_\alpha$ and model$_\beta$, respectively. The obtained trusses are fusiform shaped, i.e., the scaling ratio of the triangles peaks in the middle and vanishes at both ends. And as the external load force increases, the biggest scaling ratio increases as well, making a fatter fusiform.
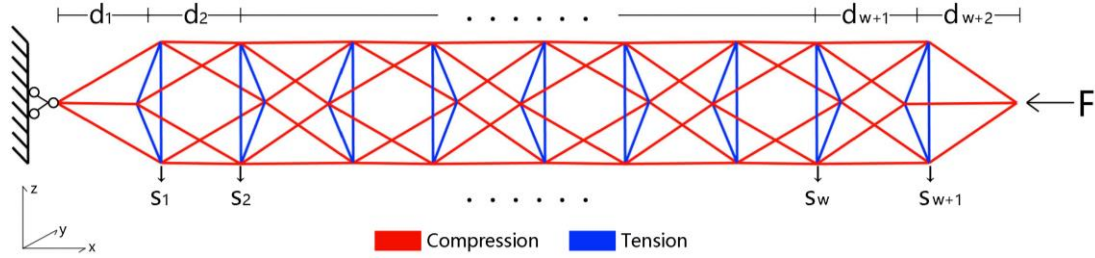

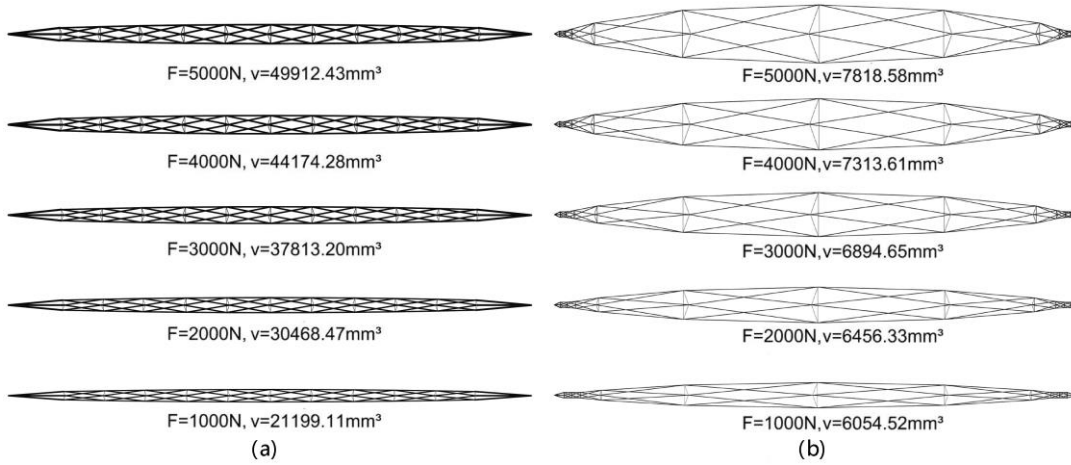Figure 2: The topology and the parametrization for the truss to be optimized.

Figure 3: Single-hierarchy truss:**(a)** trusses derived from model$_\alpha$; **(b)** trusses derived from model$_\beta$.

3.2 Case I

The experiment treats a single bar b_0 of length L=1000 mm, cross-sectional area a = 5.455 mm^2. An axial compressive load of F=3000 N is applied. The stress of the bar does not exceed the stress limit σ_0, but the bar is not stable under Euler's buckling. A solid cylindrical bar has a material volume V_0= 228225 mm^3 to be stable under load F. In this example, the single bar will be replaced with hierarchical truss structures and the obtained results will be compared with V_0.

Let T^β_0 = {b$_0$} denote the input of Algorithm2. Figure 4(a) and Figure 4(b) show the result of using the initial truss with w=10 for the first generation. The red segments denote the instable compressive members that need to be replaced. Different values of m for topology are enumerated in the optimization process of each member, and the one offering the smallest material volume is adopted. Figure 4(c) to Figure 4(e) show the structures generated from the second and third generation. The minimum bar diameter of the fourth generation is smaller than manufacturing limit, so the recursion terminates.

In the first generation, various topology with w ranging from 10 to 20 is tested. The outcome of the material volume (mm^3) is shown in Table1, along with the optimal result using Farr's algorithm [9]. The best result comes from Generation3 with w=10, which saves 92.97% of material compared to the single bar of volume V_0. Compared with the best result using Farr's method, it saves 72.54% of material.

	Farr's method	Algorithm2 Presented in Section2.3 (with compliance constraint)					
		w=10	w=12	w=14	w=16	w=18	w=20
Generation1	58416.29	37813.20	34116.98	31876.18	30689.34	30220.54	30162.73
Generation2	101522.72	19211.52	19236.81	19284.33	19546.39	20545.28	20777.01
Generation3	137111.38	16040.38	16333.41	16416.05	16634.11	16788.74	17025.10

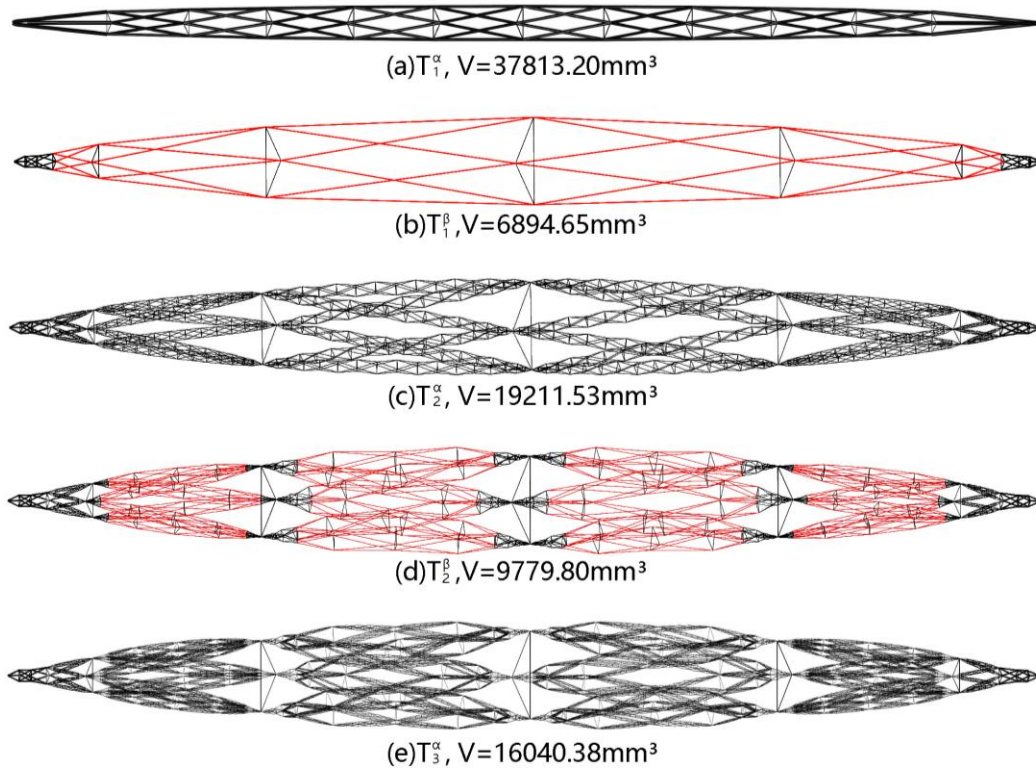Table 1: Material volume (mm^3) results of Case I.

Figure 4: Case I: recursive process of subdividing a truss (*w*=10 at the first generation) into a hierarchical truss. The red segments denote the instable compressive members that need to be further subdivided.

3.3 Case II

The second case considers the bridge structure of dimension 10 m × 1.25 m × 1 m shown in Figure 5(a). The vertical load of 80000 N is evenly distributed over 14 nodes, where each load vector is (0, 0, −5714.29 N). The compliance bound of the bridge is 1000 N· m.

In the first scenario, the positions of supported and loaded nodes are fixed; other nodes are allowed to move within a locally centered cube of side length r. We set r = 0.6m to avoid singularity (the coincidence of nodal coordinates). Figure 5(b) shows the structure derived from model$_\beta$; Figure 5(c) shows the structure by model$_\alpha$.

The second scenario allows the loaded nodes to move in the xy-plane, and the supported nodes can slide along the y-axis. The distance of their movement is limited to less than *r*. Figure 5(d) and (e) shows the optimal solutions by model$_\beta$ and model$_\alpha$, respectively.

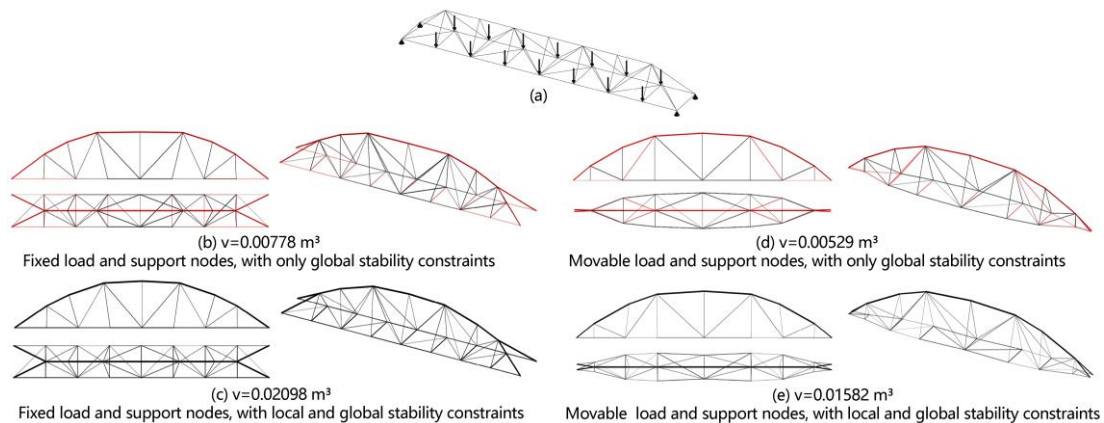Figure 5: Case II: the first hierarchy of the bridge problem. **(a)** initial topology, boundary conditions, and loads; **(b)-(e)** side, top and 3D views of the optimal designs under different configurations. The red segments denote the instable compressive bars that need to be subdivide.

Figure 6(a) depicts the optimal design by subdividing the structure in Figure 5(b) that contains 25 instable bars to be further subdivided. Because of the symmetry, only 10 out of 25 members are numbered in Figure 6(a). The data is shown in Table2, where "Stable Bar Volume" means the material volume needed for a thicker solid bar to resist Euler's buckling under the same load of the instable bar; "Truss Volume" means the material volume of the optimal hierarchical truss replacing the instable bar. The total material volume of the structure in Figure 6(a) equals to 0.00855m^3, saving 59.25% material compared with the volume of 0.02098 m^3 of the structure in Figure 5(c).
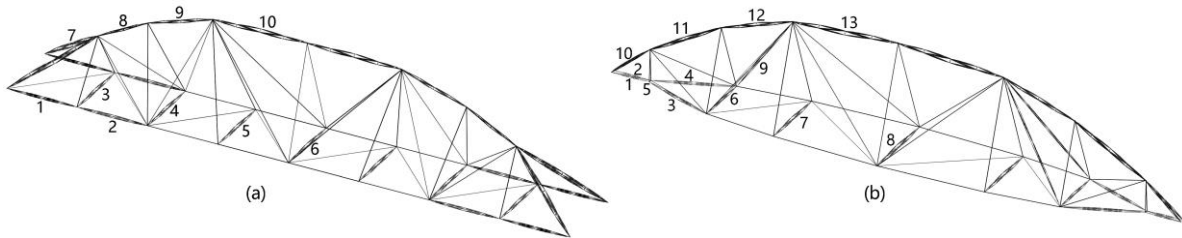

Figure 6: Case II: **(a)** the optimal design by subdividing the structure in Figure 5(b); **(b)** the optimal design by subdividing the structure in Figure 5(d).

Number	Length (mm)	Internal Force (N)	Stiffness (N/mm)	Instable Bar Volume(mm^3)	Stable Bar Volume(mm^3)	Truss Volume(mm^3)
1	1250.0	106.7	108.8	1546.7	54925.6	5227.2
2	1250.0	333.2	261.5	3715.1	97035.6	10014.6
3	1250.0	3684.6	2697.6	38319.1	322682.0	44230.8
4	1250.0	2514.6	1842.9	26178.6	266576.1	34002.4
5	1250.0	1982.7	1452.5	20632.8	236706.3	29437.6
6	1250.0	1979.5	1449.6	20591.5	236514.3	27311.0
7	1729.2	35680.1	18883.6	513312.1	1921590.5	604067.2
8	999.5	60284.1	55197.7	501300.2	834506.2	522114.2
9	1205.9	58467.5	44370.3	586611.0	1196370.7	623196.4
10	1678.3	62712.1	34197.1	875645.7	2399751.1	977904.2

Table 2: Case II: numerical data of truss members of the truss shown in Figure 6(a).

Figure 6(b) shows the optimal hierarchical structure by subdividing the structure in Figure 5(d). The material volume is 0.00601m^3, reducing 62.01% material use compared with the volume of 0.01582m^3 of the structure in Figure 5(e). The data of each truss member are presented in Table3.

Number	Length (mm)	Internal Force (N)	Stiffness (N/mm)	Instable Bar Volume(mm^3)	Stable Bar Volume(mm^3)	Truss Volume(mm^3)
1	650.1	46.9	169.0	649.3	9850.8	1646.0
2	650.1	103.5	169.0	649.3	14625.0	2089.2
3	1334.5	75.2	108.9	1763.3	52537.8	6012.3
4	1334.5	111.9	108.9	1763.3	64078.4	6910.1
5	50.0	284.6	3637.8	82.7	143.5	96.2
6	984.6	2265.8	1690.9	14901.5	156987.1	22672.4
7	1259.04	2155.3	1257.1	18115.1	250373.3	29317.0
8	1390.9	2295.4	1211.6	21309.9	315365.7	40382.1
9	2174.9	127.3	532.9	22915.0	181553.2	24379.5
10	856.8	30903.0	26539.5	177123.7	439071.0	190074.4
11	1439.9	55933.5	28520.9	537630.2	1668430.1	623696.7
12	1324.2	51341.6	28468.5	453800.5	1351723.2	535044.5
13	1853.4	51514.3	20407.9	637300.3	2652531.1	748985.3

Table 3: Case II: numerical data of truss members of the truss shown in Figure 6(b).

Figure 7: The No.7 hierarchical truss in Figure 6(a) is 3D-printed with ABS using SLA.

The No.7 member in Figure 6(a), as a hierarchical truss, is chosen to be manufactured as a 1:1 scale mock-up. This truss has a dimension of 1729.2 mm $\times$ 72.2 mm $\times$ 72.2 mm, containing 10866 bars. The compressive load along the axis of the member is 35680.1N; the compliance bound is 67.42 N· m; total volume of the structure is 604067.2 mm^3. The minimal bar diameter equals 1 mm.

Since its geometry is symmetric, half of the complex structure is fabricated using stereolithography (SLA) (Figure 7). The resolution of the 3D printing process is about 0.1 mm. Acrylonitrile Butadiene Styrene (ABS) plastic instead of the intended titanium alloy TC4 was used to reduce experimental cost. The mechanical tests will be conducted with the mock-up of titanium alloy in the future work. Due to the limited printing range of 3D metal printers, a more practical method in real world construction is to print smaller trusses at lower scale and assemble them by welding to form the upper scale truss.

4 Discussion

4.1 Limitation of the Subdivision Process

The results in Section 3 show that the recursive algorithm is more material efficient than conventional design. However, these numerical experiments have limitations.

Firstly, one particular prototype of topology (Farr's prototype [9]) is employed to replace the instable bars. The topology optimization enumerates different parameters specifying the topology. Our resultant structures are more efficient than Farr's original ones by introducing geometric optimization within each hierarchy. The proposed recursive algorithm is not limited to any particular prototype, however, a systematic construction of ideal topology for subdivision is still very much a work in progress. A more general approach would be using the ground structure method [25] instead of choosing a specific topology. But it requires a large amount of computing resources.

Secondly, the global buckling of truss structures is a nonlinear and complex process. While the prebuckling model [16] employed in this paper assumes (i) a linear relationship between the displacements and the applied loads, (ii) these displacements are orthogonal to the vector of displacements associated with global stability, and (iii) the axial forces in the bars remain constant during the deformation induced by the instability. Thus, such model is valid until the structure reaches near buckling status.

4.2 Toward Metamaterials with Additive Manufacturing

It is economical to assemble large structure with small prefabricated components in traditional hierarchical trusses. Employing structural hierarchy also reduces material use when maintaining structural stability. However, the modular members from industrial process substantially limits the

configuration space of hierarchical structures. While 3D printing naturally offers a vast design space of multiscale complex geometry. Collision between physical bars also becomes less of an issue due to the nature of additive manufacturing.

The recursive construction of hierarchical truss does not make much sense without sophisticated 3D metal printers. It is highly possible to unify high resolution printers (e.g., DMP70 of 3D MicroPrint has a resolution of 30 μm) and large-scale printers (e.g., BLT-S1500 with a 1.5 m×1.5 m×1.2 m build volume) in the next decade. At building scale, conventional welding or bolted connection can joint metal parts into larger structures. Thus, the boundary between material research and structural design is blurred. The hierarchical truss structures could be a promising prototype of the metamaterials for axial compression.

4.3 Future Works

Utilizing 3D-printed components, large-scale hierarchical trusses could find various applications in civil engineering in the near future. For practical applications, there still remain research works to be done:
(1) The uncertainty in load condition needs to be considered. Only the instable compressed bars will be subdivided into trusses at lower scale in the present algorithm, however, some tension bars may be compressed and not stable under another load condition. Therefore, multiple load cases should be introduced to improve robustness of the hierarchical truss.
(2) The resultant structures of the proposed algorithm should be compared with conventional solutions (e.g., using hollow beams, I-beams, or H-beams) to buckling problems.
(3) Mechanical tests should be conducted to verify the optimal solutions from numerical experiments.

5 Conclusions

A recursive subdivision process is proposed to construct hierarchical truss using two optimization models. From a multiscale perspective, the classic Euler buckling formula relying on the second moment of area is not always applicable at local scale, e.g., thin-walled circular tubes may experience local buckling. Thus, our model replaces instable two-force bars with fusiform trusses by a recursive construction process. The local buckling behavior characterized by Euler's critical load is transformed into the global buckling phenomenon associated with the positive semidefinite condition of the geometrical stiffness matrix.

Based on numerical experiments, the proposed optimal hierarchical truss saves around 60% of the material compared with the truss directly implemented with solid bars. A member of the structure is fabricated through 3D-printing, partially reflecting the buildability of the fractal geometry. Today, structural design can benefit from the multiscale manufacturing technology with the increasing proliferation of large-scale high-resolution3D printers, which enable a continuum differentiation from microscale to building scale. Utilizing 3D-printed metal components, the hierarchical truss could be a promising prototype for large-scale structures.

Acknowledgements

References

[1] Mandelbrot. B, *The Fractal Geometry of Nature*, Freeman, New York, 1983.
[2] Lakes. R, Materials with structural hierarchy, *Nature*, vol.361, pp. 511–515, 1993.
[3] Loyrette. H, *Gustave Eiffel*, Rizolli, New York, 1985.
[4] Harriss. J, *The Tallest Tower*, Houghton Mifflin, Boston, 1975.
[5] R. S. Farr, "Fractal design for efficient brittle plates under gentle pressure loading," *Physical* Review E, vol.76, no.4, 2007.
[6] Iasef Md Rian, "IFS-Based Computational Morphogenesis of a Hierarchical Trussed Beam,", *Proceedings of CAADFutures*, pp.996-1008, 2019.
[7] S. Asayama, T. Mae, "Fractal Truss Structure and Automatic Form Generation Using Iterated Function System", *Proceeding of ICCCBE-X*, Weimar, Germany, 2004.

[8] R. K. Daniel, Mao. Y, R. S. Farr, "Ultralight Fractal Structures from Hollow Tubes", *Physical Review Letters*, vol.109, no.12, 2012.

[9] R. S. Farr, Mao. Y, "Fractal space frames and metamaterials for high mechanical efficiency", *Europhysics Letters*, vol.84, 2008.

[10] Zheng. X, Smith. W, Jackson. J, et al, "Multiscale metallic metamaterials," *Nature Mater*, vol.15, pp.1100–1106, 2016.

[11] Wu. J, Sigmund. O, J. P. Groen. "Topology optimization of multi-scale structures: a review," *Structural and Multidisciplinary Optimization*, vol.63, pp.1455-1480, 2021.

[12] B. Jenett, C. Cameron, F. Tourlomousis, et al, "Discretely assembled mechanical metamaterials," *Science advances*, vol.6, no.47, 2020.

[13] A. Plessis, N. Razavi, M. Benedetti, et al, "Properties and applications of additively manufactured metallic cellular materials: A review," *Progress in Materials Science*, vol. 125, 2022.

[14] L. Chen, S. Liang, Y. Liu and L. Zhang, "Additive manufacturing of metallic lattice structures: Unconstrained design, accurate fabrication, fascinated performances, and challenges," *Materials Science and Engineering: R: Reports*, vol. 146, 2021.

[15] R.D. Cook, *Concepts and applications in finite element analysis*, Wiley, 1974.

[16] K.J. Bathe, *Finite element procedures in engineering analysis*, Springer, 1982.

[17] Ben-Tal A, Jarre F, Koˇcvara M, Nemirovski A, et al, "Optimal design of trusses under a nonconvex global buckling constraint," *Optimization and Engineering*, vol.1, no.2, pp.189–213, 2000.

[18] Koˇcvara M, "On the modelling and solving of the truss design problem with global stability constraints," *Structural and Multidisciplinary Optimization*, vol.23, no.3, pp.189–203, 2002.

[19] Fiala J, Koˇcvara M, Stingl M, "PENLAB: a MATLAB solver for nonlinear semidefinite optimization," 2013.

[20] D.V. Hutton, *Fundamentals of finite element analysis*, Elizabeth A. Jones, 2004.

[21] L. Euler, *A method of finding curved lines enjoying the maximum-minimum property, or the solution of the isoperimetric problem in the broadest sense*, Birkhäuser Basel, 1952.

[22] A. Tugilimana, R. F. Coelho, A. P. Thrall, "Including global stability in truss layout optimization for the conceptual design of large-scale applications," *Structural and Multidisciplinary Optimization*, vol.57, pp.1213-1233, 2018.

[23] A.G. Weldeyesus, A. Tyas, J. Gondzio, et al, "Truss geometry and topology optimization with global stability constraints," *Structural and Multidisciplinary Optimization*, vol.62, pp:1721–1737, 2020.

[24] Van Elsen. *Selective Laser Melting: a new optimization approach*, Katholieke Universiteit Leuven, 2007.

[25] Dorn W, Gomory R, Greenberg H, "Automatic design of optimal structures," *Journal de Mécanique*, vol.3, pp:25–52.